

# Fabrication and characterization of epitaxial $\text{Ba}_{0.7}\text{Sr}_{0.3}\text{TiO}_3$ thin films for optical waveguide applications

Dan-Yang Wang, Helen Lai Wa Chan, and Chung Loong Choy

The optical properties of barium strontium titanate ( $\text{Ba}_{0.7}\text{Sr}_{0.3}\text{TiO}_3$ ; BST) thin films are described. The BST thin films were epitaxially grown upon MgO (001) substrates by pulsed laser deposition. The crystallographic properties of the BST thin films were examined by x-ray diffraction. The BST thin films were highly optically transparent in the visible region. The optical waveguide properties were characterized by a prism coupling technique. An inverse-WBK method was employed to determine the refractive-index profile along the thickness of the BST films. Optical losses were measured by a moving fiber method, and the optical losses were found to be 0.93 dB/cm for the  $\text{TE}_0$  mode and 1.29 dB/cm for the  $\text{TM}_0$  mode at 1550 nm. Electro-optic (E-O) properties were measured by a phase-modulation detection method at 632.8 nm, and the BST films exhibited a predominantly quadratic E-O effect with a quadratic E-O coefficient of  $6.64 \times 10^{-18} \text{ m}^2/\text{V}^2$ . © 2006 Optical Society of America

OCIS codes: 160.2100, 230.7390, 310.6860.

## 1. Introduction

Thin-film ferroelectric oxides with excellent electro-optic (E-O) properties have attracted considerable interest in developing E-O modulators and active optical waveguides in recent years.<sup>1-4</sup> The advantage of using ferroelectric thin-film optical heterostructures includes geometrical flexibility and the ability to grow, waveguides on diverse substrates for possible integration with semiconductor lasers. Moreover, the use of thin films in E-O devices can lead to a reduction in size of devices and an increase in interaction efficiency. A variety of ferroelectric thin films have been investigated as promising candidates for E-O applications; they include lanthanum modified lead zirconate titanate, barium titanate, lead magnesium niobate-lead titanate, lithium niobate, and strontium barium niobate.<sup>5-9</sup> However, to produce high-quality thin films with good optical clarity and low optical loss for waveguide applications is still a challenging task.

Barium strontium titanate ( $\text{Ba}_{1-x}\text{Sr}_x\text{TiO}_3$ ; BST) is a well-known microwave material with a large dielectric tunability in microwave regime. Great efforts have been focused on this material for development of E-O devices in the past few years since the discovery of the promising E-O characteristics in BST thin films.<sup>10,11</sup> Thus, to fabricate high quality epitaxial BST thin films and to optimize the film performance for actual device applications have become critical objectives. Besides high E-O performance, preparation of BST thin films suitable for optical waveguiding generally requires epitaxial growth, high crystalline properties, low surface roughness, high refractive index, and low optical loss.<sup>12,13</sup> In this paper we report the fabrication and optical characterization of BST thin films epitaxially grown upon MgO (001) substrates. The nominal composition is  $\text{Ba}_{0.7}\text{Sr}_{0.3}\text{TiO}_3$ , which has a Curie point ( $T_c$ ) close to room temperature and has a high dielectric constant and wide tunability<sup>14</sup>; thus a good E-O property is expected.

## 2. Experiment

A pulsed laser deposition (PLD) technique was employed to produce epitaxial  $\text{Ba}_{0.7}\text{Sr}_{0.3}\text{TiO}_3$  thin films.  $\text{Ba}_{0.7}\text{Sr}_{0.3}\text{TiO}_3$  films of approximately 250 and 620 nm thickness were grown upon cubic MgO (001) single-crystal substrates polished on both sides by irradiating the stoichiometric target with a laser beam of 248 nm wavelength and 25 ns pulse duration from a

---

The authors are with the Department of Applied Physics and Material Research Centre, The Hong Kong Polytechnic University, Hung Hom, Kowloon, Hong Kong, China. D.-Y. Wang's e-mail address is 0201276r@polyu.edu.hk.

Received 24 January 2005; accepted 10 October 2005.

0003-6935/06/091972-07\$15.00/0

© 2006 Optical Society of America

Table 1. PLD Conditions of Ba<sub>0.7</sub>Sr<sub>0.3</sub>TiO<sub>3</sub> Thin Films

Target–substrate distance (mm)	50
Laser energy (mJ)	250
Repetition rate of pulsed laser (Hz)	10
Ambient gas	O <sub>2</sub>
Total pressure of ambient gas (mTorr)	200
Substrate temperature (°C)	650
Growth rate (nm/min)	~20

KrF excimer laser (Lambda Physik COMPex 250). The pulse energy of the laser beam was 250 mJ, and the repetition rate was 10 Hz. The distance between the target and the substrates was fixed at 5 cm. The substrate temperature was maintained at 650 °C. The oxygen partial pressure was kept at 200 mTorr during laser ablation. The PLD conditions are summarized in Table 1. After deposition, the films were postannealed at 1000 °C in a tube furnace for 3 h.

The crystal structure of the BST thin films was examined with an x-ray diffractometer (Bruker D8 Discover) equipped with Cu K<sub>α</sub> radiation. The surface morphology of the thin films was observed with an atomic-force microscope (AFM; Digital Instruments NanoScope IV) working in a tapping mode. The optical transmission of the BST thin films was measured with a transmission-type ellipsometer (Jobin Yvon UVISEL) in the wavelength range 280–850 nm. The waveguide properties and optical loss of the BST films were measured with a prism coupler (Metricon 2010) at both 632.8 and 1550 nm.

For E-O measurement, a layer of gold of 200 nm thickness was deposited upon the surface of the film by rf magnetron sputtering, followed by standard photolithography and wet chemical etching to form coplanar electrodes with a gap of 40 μm. The E-O properties of the thin films were measured at a fixed wavelength of 632.8 nm by the phase-modulation detection method with an ellipsometer (Jobin Yvon UVISEL) working in transmission mode. Details of this method were presented previously.<sup>15</sup>

### 3. Results and Discussion

Figure 1(a) shows the typical θ/2θ x-ray diffraction (XRD) patterns of a 250 nm thick Ba<sub>0.7</sub>Sr<sub>0.3</sub>TiO<sub>3</sub> thin film deposited upon a MgO (001) substrate. Only (001) peaks appear in the XRD pattern, indicating that the BST thin film has a single perovskite phase with its *c* axes normal to the substrate surface, or <001><sub>BST</sub>//<001><sub>MgO</sub>. The out-of-plane and in-plane lattice parameters were calculated to be *c* = 3.9751 Å and *a* = 4.0003 Å, respectively (1 Å = 0.1 nm), implying that the film is under biaxial tensile strain. (Lattice parameters of MgO and Ba<sub>0.7</sub>Sr<sub>0.3</sub>TiO<sub>3</sub> ceramics are 4.215 Å and 3.970 Å, respectively). The rocking curve measurements from the (002) reflections reveal that the value of the FWHM is ~0.90°, as shown in Fig. 1(a), inset. The small FWHM value suggests that the Ba<sub>0.7</sub>Sr<sub>0.3</sub>TiO<sub>3</sub> film has good single-crystal quality. We performed an off-axis φ scan of

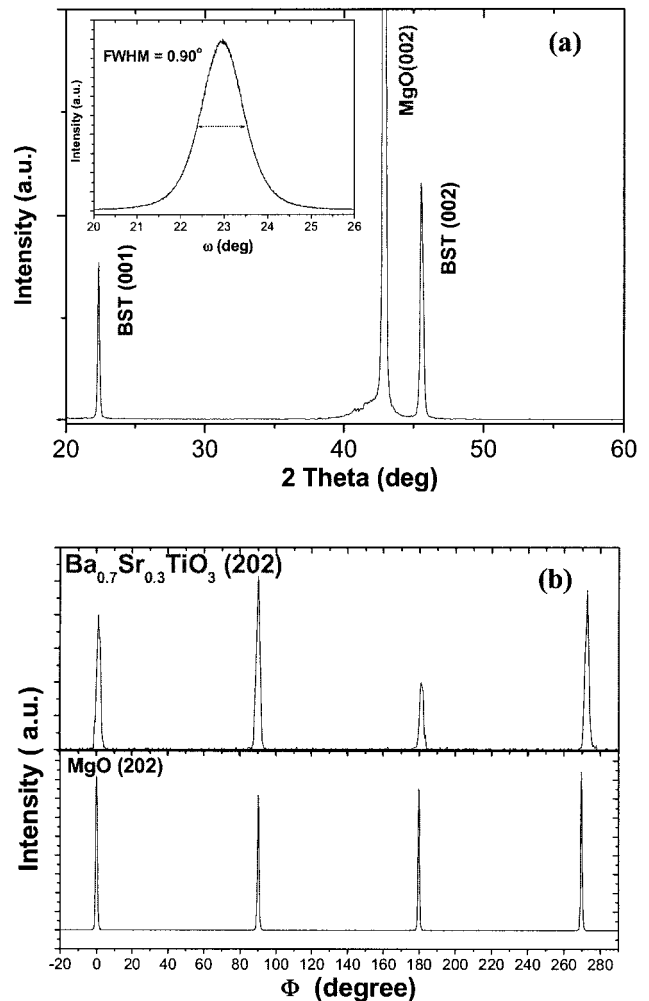


Fig. 1. XRD patterns of Ba<sub>0.7</sub>Sr<sub>0.3</sub>TiO<sub>3</sub> thin film: (a) θ/2θ scan [inset, rocking curve of the (002) peak]; (b) φ scan of (202) reflections of the Ba<sub>0.7</sub>Sr<sub>0.3</sub>TiO<sub>3</sub> thin film.

(202) reflections of the Ba<sub>0.7</sub>Sr<sub>0.3</sub>TiO<sub>3</sub> thin film to understand the quality of epitaxy and to determine the in-plane relationship between the BST film and the MgO substrate. As shown in Fig. 1(b), the fourfold symmetric (202) reflections of BST film are very sharp and coincide well with those of the MgO substrate, suggesting that the BST film has a high degree of in-plane orientation and a cube-on-cube epitaxial growth upon a MgO (001) substrate. The in-plane orientation relationship has been determined to be <100><sub>BST</sub>//<100><sub>MgO</sub>. For optical applications, such uniformly aligned crystal grains in an epitaxially grown film are highly desirable.

The surface morphology and roughness of the epitaxial Ba<sub>0.7</sub>Sr<sub>0.3</sub>TiO<sub>3</sub> thin film are shown in the AFM image in Fig. 2. The average grain size was estimated to range from 80 to 120 nm in diameter. The AFM image reveals that the BST thin film has a smooth and dense surface. The root-mean-square roughness is ~3.4 nm over 1 μm × 1 μm area of the 250 nm thick film. Some authors have proposed a relationship between the film's microstructure and optical

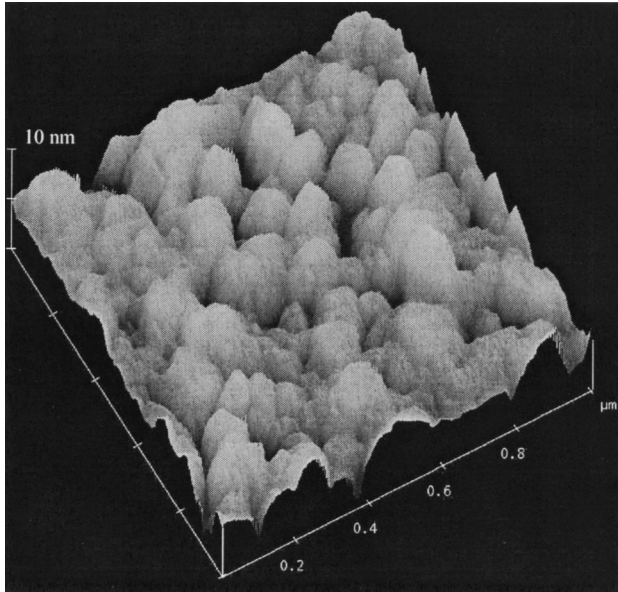


Fig. 2. AFM image taken from a 250 nm thick  $\text{Ba}_{0.7}\text{Sr}_{0.3}\text{TiO}_3$  thin film epitaxially grown upon a MgO (001) substrate.

properties. Wessels *et al.*<sup>16</sup> studied the effect of surface roughness on light scattering for ferroelectric oxide films, and they suggested that the surface roughness requirements may be 2–4 nm to produce low optical scattering losses of 1–2 dB/cm. The roughness of our BST films is within the optimum range, so a low optical loss is expected.

The optical transmission of the  $\text{Ba}_{0.7}\text{Sr}_{0.3}\text{TiO}_3$  thin film (250 nm thick) in the wavelength range 280–850 nm is shown in Fig. 3(a). The films are highly transparent in the visible region, with transmittance from 58% to 90%. The transparency of the film drops sharply in the UV region, and the threshold wavelength is located at 316 nm. The optical bandgap energy  $E_{\text{gap}}$  of a thin film can be deduced from the spectral dependence of absorption constant  $\alpha(\nu)$  by application of the Tauc relation<sup>17</sup>

$$\alpha h\nu = \text{const.} (h\nu - E_{\text{gap}})^{1/r}, \quad (1)$$

where  $\nu$  is the frequency,  $h$  is Planck's constant, and  $r = 2$  for a direct allowed transition.

Absorption constant  $\alpha(\nu)$  is determined from the transmittance spectrum from the relation<sup>17</sup>

$$\alpha(\nu) = \left[ \ln \frac{1}{T(\nu)} \right] / d, \quad (2)$$

where  $T(\nu)$  is the transmittance at frequency  $\nu$  and  $d$  is the film thickness. The optical bandgap energy is then obtained from Eq. (1) by extrapolation of the linear portion of the plot of  $(\alpha h\nu)^2$  versus  $h\nu$  to  $(\alpha h\nu)^2 = 0$ . Figure 3(b) shows  $(\alpha h\nu)^2$  versus  $h\nu$  for  $\text{Ba}_{0.7}\text{Sr}_{0.3}\text{TiO}_3$  film grown upon a MgO substrate. The optical bandgap energy was found to be 3.50 eV for the  $\text{Ba}_{0.7}\text{Sr}_{0.3}\text{TiO}_3$  thin film.

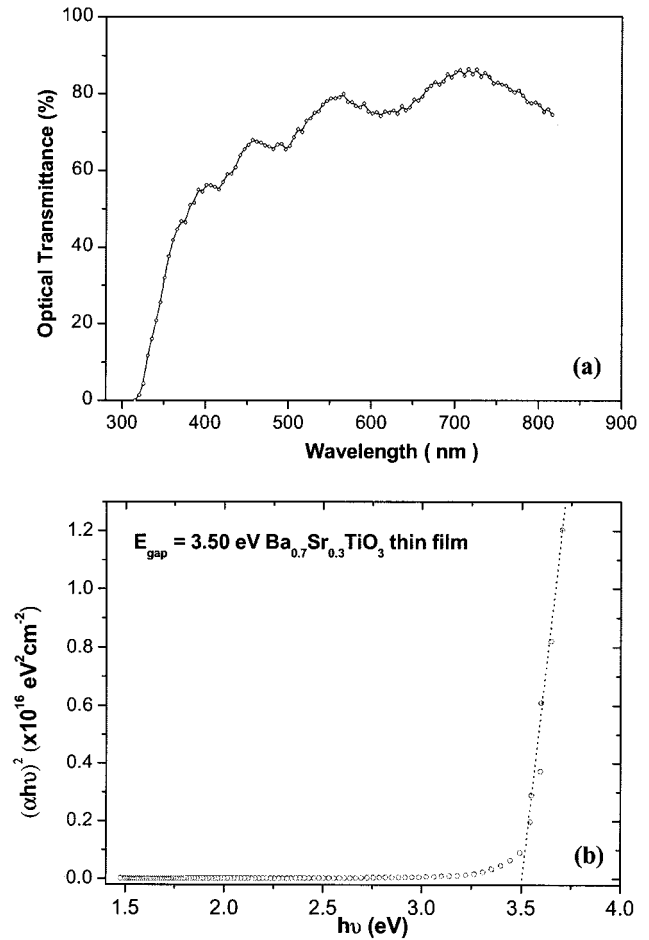


Fig. 3. (a) Optical transmission spectrum of a  $\text{Ba}_{0.7}\text{Sr}_{0.3}\text{TiO}_3$  thin film (250 nm thick) epitaxially grown upon a MgO (001) substrate, (b) plot of  $(\alpha h\nu)^2$  versus  $h\nu$  for a  $\text{Ba}_{0.7}\text{Sr}_{0.3}\text{TiO}_3$  thin film (250 nm thick). Optical bandgap energy  $E_{\text{gap}}$  is deduced from extrapolation of the straight line to  $(\alpha h\nu)^2 = 0$ .

To characterize the waveguide properties of the  $\text{Ba}_{0.7}\text{Sr}_{0.3}\text{TiO}_3$  films we performed prism coupling experiments at both 632.8 and 1550 nm. Figure 4 shows the guided-mode spectra ( $m$ -lines) of a 620 nm thick  $\text{Ba}_{0.7}\text{Sr}_{0.3}\text{TiO}_3$  thin film upon a MgO (001) substrate measured by the prism coupler. Three TE (transverse electric) and three TM (transverse magnetic) modes were observed at 632.8 nm, while only a single TE and a single TM mode were found at 1550 nm. The peak of each guided mode is sharp and distinguishable, indicating that a good confinement of light propagation is achieved and the film is potentially useful for optical waveguide devices. The measured film thickness of 626.0 nm in the TE mode at 632.8 nm was in good agreement with that determined by an  $\alpha$ -step profile measurement. At a wavelength of 632.8 nm the refractive indices for TE and TM modes were determined to be 2.1696 and 2.2185, respectively, giving an index difference of 0.0489. The large index difference cannot be fully explained by the intrinsic birefringence in the film and may be due to the lattice-mismatch-induced strain, as presented in the analysis of XRD results. Because the  $m$ -lines ap-

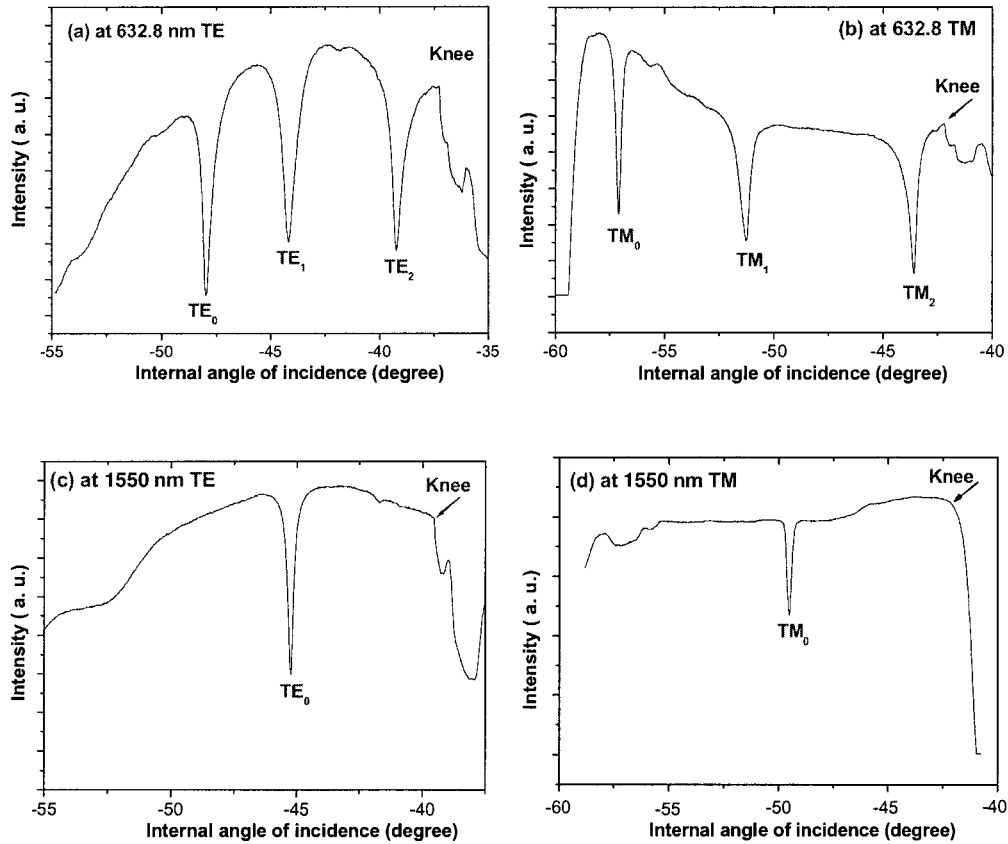


Fig. 4. Prism coupling spectra of a  $\text{Ba}_{0.7}\text{Sr}_{0.3}\text{TiO}_3$  thin film (620 nm thick) epitaxially grown upon a MgO (001) substrate at both 632.8 and 1550 nm.

peared well defined and relatively sharp, it can be supposed that the optical losses in the film are rather low because the optical losses are related to the FWHM of the  $m$ -lines.<sup>13,18</sup> It is obvious that the FWHM of  $m$ -lines at 1550 nm is smaller than that at 632.8 nm; a lower optical loss is expected at 1550 nm.

From knowledge of the effective mode indices it is possible to determine the refractive-index profile along the film thickness direction for either the TE or the TM mode by using the inverse Wentzel-Kramers-Brillouin ( $i$ -WKB) method, which was previously introduced by Chiang.<sup>19</sup> This method depends only on the refractive-index distribution within the guiding layer. The refractive-index profile of the  $\text{Ba}_{0.7}\text{Sr}_{0.3}\text{TiO}_3$  thin film at 632.8 nm is shown in Fig. 5. It indicates a steplike index variation, which is synonymous with good optical homogeneity along the BST film thickness. The refractive index remains constant within the guiding region and drops rapidly near the film-substrate interface. This is so because plenty of lattice-misfit-induced dislocations exist near the film-substrate interface,<sup>20</sup> thus degrading the optical properties at the interface.

Optical clarity is a demanding requirement for thin-film waveguides, and the optical losses are a major barrier to using ferroelectric thin films in waveguide applications. A loss of  $\sim 2$  dB/cm will reduce the efficiency of an optical device (e.g., a fre-

quency doubler) by more than 50%.<sup>21</sup> Nevertheless, investigations of the optical losses in ferroelectric thin films are insufficient. The optical loss has several causes, including absorption, mode leakage, internal scattering, and surface scattering. For a transparent ferroelectric thin film the dominant loss mechanism is scattering.<sup>7</sup> In this study we employed a moving

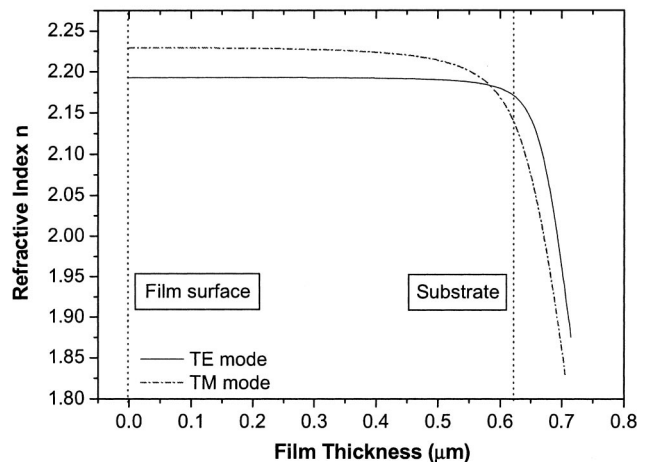


Fig. 5. Reconstruction of the refractive-index profile of the  $\text{Ba}_{0.7}\text{Sr}_{0.3}\text{TiO}_3$  thin film (620 nm thick) epitaxially grown upon a MgO (001) substrate at 632.8 nm by use of an  $i$ -WKB method.



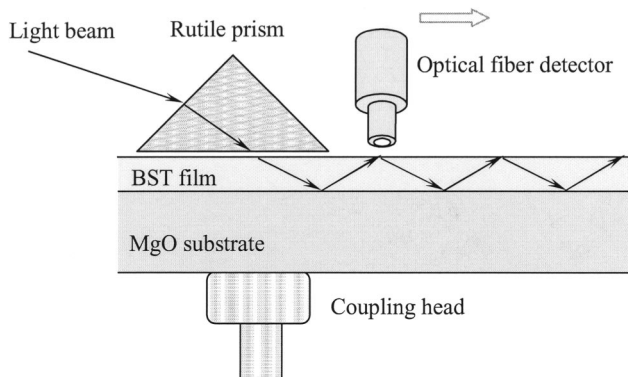


Fig. 6. Schematic diagram of the experimental arrangement for measurements of surface scattering loss (moving fiber method).

fiber method (build-in options of the Metricon 2010 prism coupler) to determine the surface scattering losses in the  $\text{Ba}_{0.7}\text{Sr}_{0.3}\text{TiO}_3$  thin film (620 nm thick). The measurement setup is shown schematically in Fig. 6. In the moving fiber method, the exponential decay of light is measured by a fiber probe scanning the length of the propagating streak. The optical fiber method is identical in concept to the CCD camera approach for measuring the decay of the propagating streak as described previously.<sup>7,22</sup> The loss was derived for the film from measurements of the out-of-plane scattered light intensity for the specified guiding modes. Figure 7 shows the scattered intensity from  $\text{TE}_0$  and  $\text{TM}_0$  modes at both 632.8 and 1550 nm. A least-squares fit gives losses of 2.64 and 3.04 dB/cm for  $\text{TE}_0$  and  $\text{TM}_0$  modes, respectively, at 632.8 nm and of 0.93 and 1.29 dB/cm for  $\text{TE}_0$  and  $\text{TM}_0$  modes at 1550 nm. Losses with similar magnitude were measured for the other guided modes of the  $\text{Ba}_{0.7}\text{Sr}_{0.3}\text{TiO}_3$  thin film, as summarized in Table 2. For modes of higher order, higher scattered losses were observed. It is noticeable that the scattered losses at 1550 nm, the commonly used wavelength in optical communication, are rather low, consistent with our prediction using AFM image and  $m$ -line measurements. The accuracy of our loss results is limited because of the small sample area and thus the short scanning length along the light propagation direction. But it gives a good approximation, and the results are comparable with previously reported data for ferroelectric thin films.<sup>7,12,22</sup>

The electro-optic properties of the  $\text{Ba}_{0.7}\text{Sr}_{0.3}\text{TiO}_3$  thin films were measured with transverse geometry at a wavelength of 632.8 nm by the phase-modulation detection method.<sup>15</sup> The field-induced birefringence of the  $\text{Ba}_{0.7}\text{Sr}_{0.3}\text{TiO}_3$  thin film (~250 nm thick) was measured as a function of dc electric field  $E$  at room temperature, and the result is shown in Fig. 8(a). A similar electrode pattern was also deposited upon a MgO substrate and, on application of a dc field,  $\Delta n = 0$  was observed (not shown here). This result implies that the change in birefringence observed in the BST-MgO structure originated from the BST thin film. Figure 8(b) shows a plot of birefringence shift  $\Delta n$  versus  $E^2$  for the  $\text{Ba}_{0.7}\text{Sr}_{0.3}\text{TiO}_3$  thin film, and it can

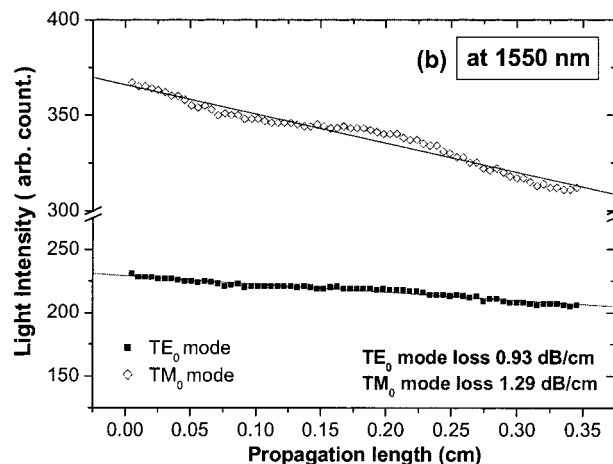
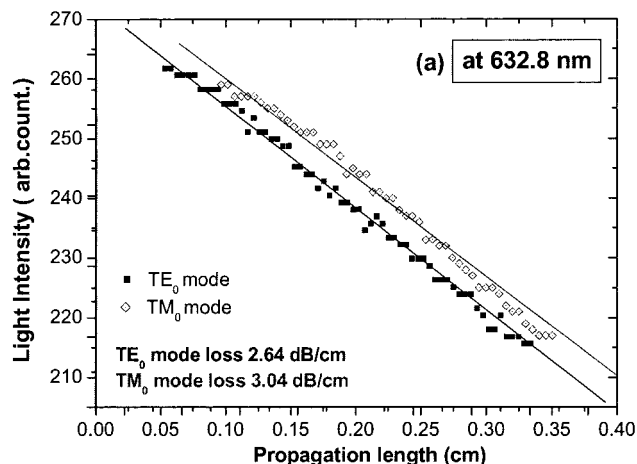


Fig. 7. Scattered intensity from the  $\text{TE}_0$  and  $\text{TM}_0$  modes of a 620 nm thick  $\text{Ba}_{0.7}\text{Sr}_{0.3}\text{TiO}_3$  thin film epitaxially grown on MgO (001) substrate at both 632.8 nm and 1550 nm.

be seen that  $\Delta n$  varies linearly with  $E^2$ . Quadratic electro-optic coefficient  $R$  is defined by the equation<sup>23</sup>

$$\Delta n = -\frac{1}{2}n^3RE^2, \quad (3)$$

where  $\Delta n$  is the birefringence and  $n$  is the refractive index (taken as 2.2 for BST). Using Eq. (3), we calculated the quadratic E-O coefficient  $R$  to be

Table 2. Surface Scattered Losses in  $\text{Ba}_{0.7}\text{Sr}_{0.3}\text{TiO}_3$  Thin Films Epitaxially Grown Upon MgO (001) Substrates

Guided Mode	Loss	
	At 632.8 nm (dB/cm)	At 1550 nm (dB/cm)
$\text{TE}_0$	2.64	0.93
$\text{TE}_1$	6.43	
$\text{TE}_2$	8.33	
$\text{TM}_0$	3.04	1.29
$\text{TM}_1$	5.39	
$\text{TM}_2$	8.85	

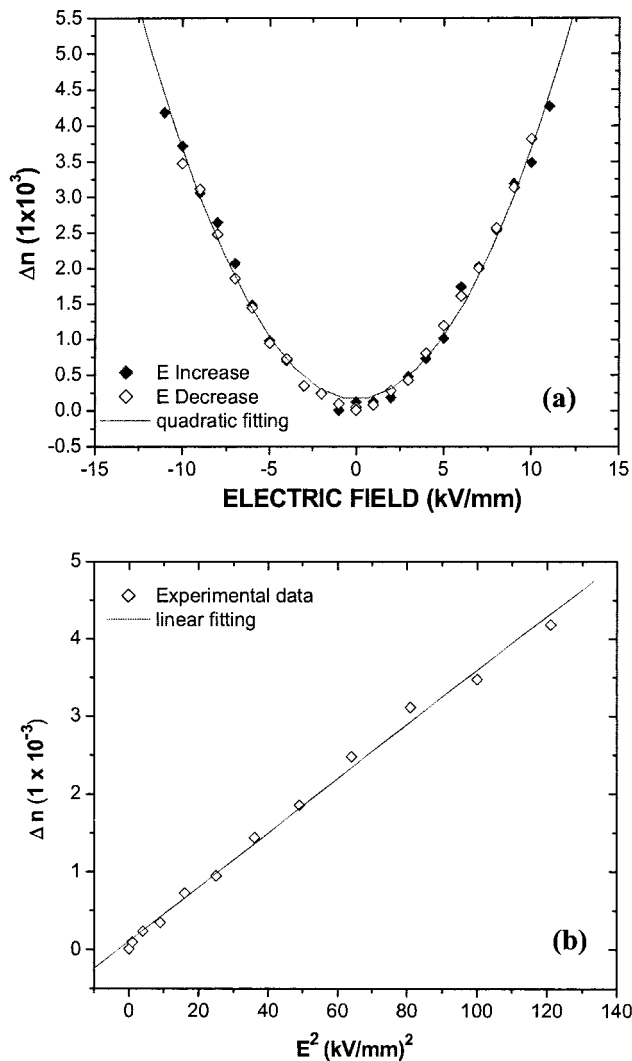


Fig. 8. (a) Electro-optic responses of the  $\text{Ba}_{0.7}\text{Sr}_{0.3}\text{TiO}_3$  thin film (250 nm thick) epitaxially grown upon a MgO (001) substrate, (b) electro-optic response versus  $E^2$  of the  $\text{Ba}_{0.7}\text{Sr}_{0.3}\text{TiO}_3$  thin film.

$6.64 \times 10^{-18} \text{ m}^2/\text{V}^2$ . This value is comparable to the E-O coefficients of ferroelectric relaxor lead zirconate titanate thin films.<sup>24</sup>

#### 4. Conclusions

In summary, high-quality  $\text{Ba}_{0.7}\text{Sr}_{0.3}\text{TiO}_3$  thin films have been deposited upon MgO (001) substrates by pulsed laser deposition. XRD examination revealed an epitaxial growth and a pure perovskite phase with good single-crystal quality. AFM observation exhibited a smooth film surface with a root-mean-square roughness of  $\sim 3.4$  nm. The optical properties of the BST films were found to have potential for waveguide applications. The films possess good optical clarity with high optical transmission in visible portion of the spectrum. The waveguide characteristics of the BST films were determined by a prism coupling technique. We found good optical homogeneity of the films along the thickness direction by analyzing the guided-mode spectra, using the *i*-WKB method. The

BST films showed relatively low surface scattered losses of 0.93 and 1.29 dB/cm for  $\text{TE}_0$  and  $\text{TM}_0$  modes, respectively, at 1550 nm, values that are suitable for use in infrared waveguides. A quadratic E-O coefficient of  $R = 6.64 \times 10^{-18} \text{ m}^2/\text{V}^2$  was found in the BST thin films. Our future research will aim at the fabrication and characterization of ridge waveguides and Mach-Zehnder interferometers by use of BST thin films.

The authors thank S. G. Lu for his help in PLD target preparation. Financial support from the Centre for Smart Materials of the Hong Kong Polytechnic University is acknowledged.

#### References

1. H. Adachi and K. Wasa, "Sputtering preparation of ferroelectric PLZT thin films and their optical applications," *IEEE Trans. Ultrason. Ferroelectr. Freq. Control* **38**, 645–655 (1991).
2. A. Petraru, J. Schubert, M. Schmid, and Ch. Buchal, "Ferroelectric  $\text{BaTiO}_3$  thin-film optical waveguide modulators," *Appl. Phys. Lett.* **81**, 1375–1377 (2002).
3. M. Blomqvist, S. Khartsev, A. Crishin, A. Petraru, and C. Buchal, "Optical waveguiding in magnetron-sputtered  $\text{Na}_{0.5}\text{K}_{0.5}\text{NbO}_3$  thin films on sapphire substrates," *Appl. Phys. Lett.* **82**, 439–441 (2003).
4. D. M. Gill, B. A. Block, C. W. Conrad, B. W. Wessels, and S. T. Ho, "Thin film channel waveguides fabricated in metalorganic chemical vapor deposition grown  $\text{BaTiO}_3$  on  $\text{MgO}$ ," *Appl. Phys. Lett.* **69**, 2968–2970 (1996).
5. H. Adachi, T. Mitsuyu, O. Yamazaki, and K. Wasa, "Ferroelectric (Pb, La)(Zr, Ti) $\text{O}_3$  epitaxial thin films on sapphire grown by rf-planar magnetron sputtering," *J. Appl. Phys.* **60**, 736–741 (1986).
6. D. H. Kim and H. S. Kwok, "Pulsed laser deposition of  $\text{BaTiO}_3$  thin films and their optical properties," *Appl. Phys. Lett.* **67**, 1803–1805 (1995).
7. Y. Lu, G.-H. Jin, M. Cronin-Golomb, S.-W. Liu, H. Jiang, F.-L. Wang, J. Zhao, S.-Q. Wang, and A. J. Drehman, "Fabrication and optical characterization of  $\text{Pb}(\text{Mg}_{1/3}\text{Nb}_{2/3})\text{O}_3$ - $\text{PbTiO}_3$  planar thin film optical waveguides," *Appl. Phys. Lett.* **72**, 2927–2929 (1998).
8. D. W. Kim, S. H. Lee, and T. W. Noh, "Structural and nonlinear optical properties of epitaxial  $\text{LiNbO}_3$  films grown by pulsed laser deposition," *Mater. Sci. Eng. B* **56**, 251–255 (1998).
9. L. D. Zhu, J. Zhao, F. Wang, P. E. Norris, G. D. Fogarty, B. Steiner, P. Lu, B. Kear, S. B. Kang, B. Gallois, M. Sinclair, D. Dimos, and M. Cronin-Golomb, "Epitaxial electro-optical  $\text{Sr}_x\text{Ba}_{1-x}\text{Nb}_2\text{O}_6$  films by single-source plasma-enhanced metalorganic chemical vapor deposition," *Appl. Phys. Lett.* **67**, 1836–1838 (1995).
10. D.-Y. Kim, S. E. Moon, E.-K. Kim, S.-J. Lee, J.-J. Choi, and H. E. Kim, "Electro-optic characterization of (001)-oriented  $\text{Ba}_{0.6}\text{Sr}_{0.4}\text{TiO}_3$  thin films," *Appl. Phys. Lett.* **82**, 1455–1457 (2003).
11. J. Li, F. Duewer, C. Gao, H. Chang, X.-D. Xiang, and Y. Lu, "Electro-optic measurements of the ferroelectric-paraelectric boundary in  $\text{Ba}_{1-x}\text{Sr}_x\text{TiO}_3$  materials chips," *Appl. Phys. Lett.* **76**, 769–771 (2000).
12. L. Beckers, J. Schubert, W. Zander, J. Ziesmann, A. Echau, P. Leinenbach, and Ch. Buchal, "Structural and optical characterization of epitaxial waveguiding  $\text{BaTiO}_3$  thin films on  $\text{MgO}$ ," *J. Appl. Phys.* **83**, 3305–3310 (1998).

13. B. Vilquin, R. Bouregba, G. Poullain, H. Murray, E. Dogheche, and D. Remiens, "Crystallographic and optical properties of epitaxial  $\text{Pb}(\text{Zr}_{0.6}, \text{Ti}_{0.4})\text{O}_3$  thin films grown on  $\text{LaAlO}_3$  substrates," *J. Appl. Phys.* **94**, 5167–5171 (2003).
14. Y. Lin, J.-Sik Lee, H. Wang, Y. Li, S. R. Foltyn, Q. X. Jia, G. E. Collis, A. K. Burrell, and T. M. McCleskey, "Structural and dielectric properties of epitaxial  $\text{Ba}_{1-x}\text{Sr}_x\text{TiO}_3$  films grown on  $\text{LaAlO}_3$  substrates by polymer-assisted deposition," *Appl. Phys. Lett.* **85**, 5007–5009 (2004).
15. D. Y. Wang, C. L. Mak, K. H. Wong, H. L. W. Chan, and C. L. Choy, "Optical properties of  $\text{Ba}_{0.5}\text{Sr}_{0.5}\text{TiO}_3$  thin films grown on  $\text{MgO}$  substrates by pulsed laser deposition," *Ceramurgia Int.* **30**, 1745–1748 (2004).
16. B. W. Wessels, M. J. Nystrom, J. Chen, D. Studebaker, and T. J. Marks, "Epitaxial niobate thin films and their nonlinear optical properties," *Mater. Res. Soc. Symp. Proc.* **401**, 211–218 (1996).
17. H. Y. Tian, W. G. Luo, X. H. Pu, X. Y. He, P. S. Qiu, A. L. Ding, S. H. Yang, and D. Mo, "Determination of the optical properties of sol-gel-derived  $\text{Ba}_x\text{Sr}_{1-x}\text{TiO}_3$  thin films by spectroscopic ellipsometry," *J. Phys Condens. Matter* **13**, 4065–4073 (2001).
18. E. Dogheche, X. Lansiaux, and D. Remiens, "m-line spectroscopy for optical analysis of thick  $\text{LiNbO}_3$  layers grown on sapphire substrates by radio-frequency multistep sputtering," *J. Appl. Phys.* **93**, 1165–1168 (2003).
19. K. S. Chiang, "Construction of refractive index profiles of planar dielectric waveguides from the distribution of effective indexes," *J. Lightwave Technol.* **3**, 385–391 (1985).
20. C. L. Chen, T. Garret, Y. Lin, J. C. Jiang, E. I. Meletis, F. A. Miranda, Z. Zhang, and W. K. Chu, "Interface structures and epitaxial behavior of ferroelectric ( $\text{Ba}$ ,  $\text{Sr}$ ) $\text{TiO}_3$  thin films," *Integr. Ferroelectr.* **42**, 165–172 (2002).
21. D. K. Fork, F. Armani-Leplingard, and J. J. Kingston, "Optical losses in ferroelectric oxide thin films: Is there light at the end of the tunnel?" *Mater. Res. Soc. Symp. Proc.* **361**, 155–166 (1995).
22. F. J. Walker, R. A. McKee, H.-Wun Yen, and D. E. Zelmon, "Optical clarity and waveguide performance of thin film perovskites on  $\text{MgO}$ ," *Appl. Phys. Lett.* **65**, 1495–1497 (1994).
23. G. H. Haertling, "Ferroelectric ceramics: history and technology," *J. Am. Ceram. Soc.* **82**, 797–818 (1999).
24. A. Y. Wu, F. Wang, C. Juang, C. Bustmante, C. Yeh, and J. Diels, "Electro-optic and non-linear optical properties on ( $\text{Pb}$ ,  $\text{La}$ )( $\text{Zr}$ ,  $\text{Ti}$ ) $\text{O}_3$ ,  $\text{BaTiO}_3$ , ( $\text{Sr}$ ,  $\text{Ba}$ ) $\text{Nb}_2\text{O}_6$ ,  $\text{Ba}_2\text{NaNb}_5\text{O}_{15}$ , and beta- $\text{BaB}_2\text{O}_4$  thin films," in *Proceedings of the IEEE 7th International Symposium on Applied Ferroelectronics* (Institute of Electrical and Electronics Engineers, 1990), p. 135.